How to cite: *Angew. Chem. Int. Ed.* **2022,** *61,* e202205277
International Edition: doi.org/10.1002/anie.202205277
German Edition: doi.org/10.1002/ange.202205277

Fluorination **Hot Paper**

Stereocontrolled Synthesis of Fluorinated Isochromans via Iodine(I)/Iodine(III) Catalysis

*Joel Häfliger, Olga O. Sokolova, Madina Lenz, Constantin G. Daniliuc, and Ryan Gilmour**

Dedicated to Professor David O'Hagan on the occasion of his 60th birthday

Abstract: The success of saturated, fluorinated heterocycles in contemporary drug discovery provides a stimulus for creative endeavor in main group catalysis. Motivated by the ubiquity of isochromans across the bioactive small molecule spectrum, the prominence of the anomeric effect in regulating conformation, and the metabolic lability of the benzylic position, iodine(I)/iodine(III) catalysis has been leveraged for the stereocontrolled generation of selectively fluorinated analogs. To augment the current arsenal of fluorocyclization reactions involving carboxylic acid derivatives, the reaction of readily accessible 2-vinyl benzaldehydes is disclosed (up to >95:05 *d.r.* and 97:03 *e.r.*). Key stereoelectronic interactions manifest themselves in the X-ray crystal structures of the products, thereby validating the [CH_2-CHF] fragment as a stereoelectronic mimic of the [O-CH(OR)] acetal motif.

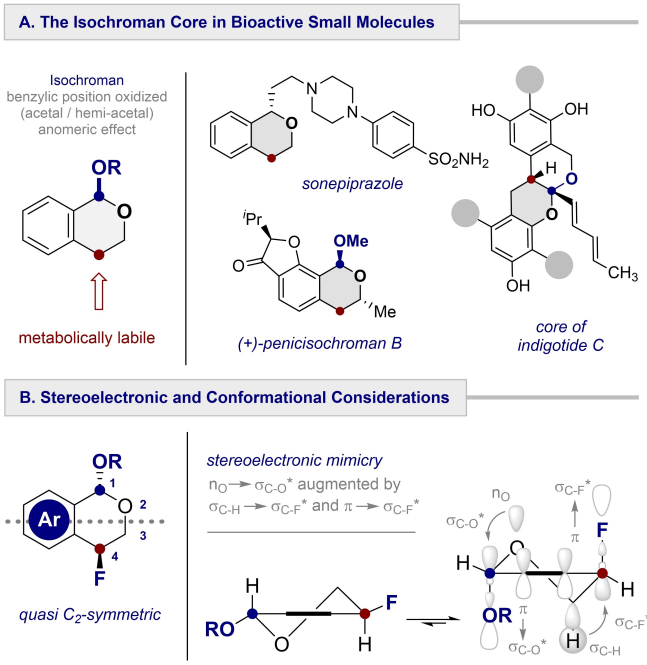

Figure 1. Bioactive isochromans and stereoelectronic mimicry and bioisostere design.

Introduction

Saturated fluorinated heterocycles are projected to play an increasingly important role in 3D chemical space exploration for drug discovery.[1,2] This is a logical consequence of "*escaping flatland*" in the pursuit of innovative structural modules,[3] merged with the historic success of fluorination tactics in regulating physicochemical properties.[1c,4] Main group fluorination platforms[5] provide an opportunity for creative endeavour in converting simple, abundant precursors into next generation pharmacophores. Motivated by the ubiquity of isochromans across the bioactive small molecule repertoire (Figure 1A),[6] it was envisaged that routes to optically active, fluorinated isosteres would be highly enabling.[1e,7] This structural unit is frequently oxidized to the benzylic (hemi)acetal, where the anomeric effect ($n_O \rightarrow \sigma_{C-O}^*$) influences the half-chair conformer population.[8] Cognizant of the metabolic liability of benzylic C(sp^3)–H bonds, stereoselective (1,4-*trans*) fluorination of the antipodal position would shield this site from undesired oxidation, and also reinforce the intrinsic conformational preference of the native heterocycle (Figure 1B). The creation of a *quasi*-C_2 symmetric system,[9] where $\sigma_{C-H} \rightarrow \sigma_{C-F}^*$ and $\pi \rightarrow \sigma_{C-F}^*$[10] interactions would support the anomeric effect, would allow the CH_2–CHF fragment to be validated as a stereoelectronic mimic of the O–CH(OR) motif.

Leveraging I^I/I^{III} catalysis,[5,11] it was posited that an alkene activation/fluorination sequence[12] of 2-vinylbenzaldehydes would trigger cyclization: importantly, this hypervalent iodine strategy would mitigate acid-catalyzed Prins-type reactivity. Subsequent diastereoselective addition of an external alcohol to the transient oxocarbenium ion would generate the desired isochroman isostere containing two

[*] J. Häfliger, Dr. O. O. Sokolova, M. Lenz, Dr. C. G. Daniliuc, Prof. Dr. R. Gilmour
Organisch-Chemisches Institut, Westfälische Wilhelms-Universität Münster
Corrensstraße 36, 48149 Münster (Germany)
E-mail: ryan.gilmour@uni-muenster.de
Homepage: https://www.uni-muenster.de/Chemie.oc/gilmour/

stereogenic centers, enabling the creation of three new σ-bonds in a single operation (Scheme 1). This would complement the carboxylic acid-based fluorocyclization repertoire[12] to include aldehydes. Confidence in this intermolecular capture strategy stemmed from the seminal work of Matviitsuk and Denmark in which highly selective sulfenoacetalization of alkenyl aldehydes was achieved under Lewis base catalysis.[13] Importantly, this strategy would complement heteroarene hydrogenation approaches to saturated mono-fluorinated heterocycles by expanding beyond the *cis*-stereochemical limitations.[14]

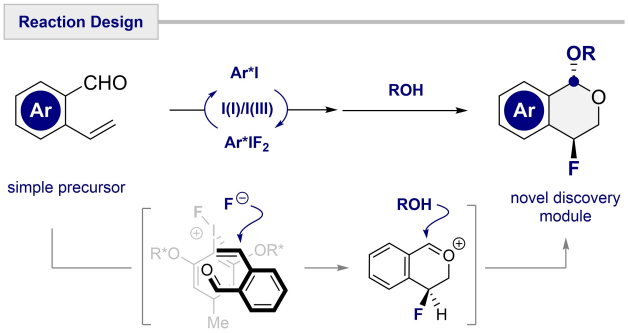

Scheme 1. An I^{I}/I^{III} catalysis route to fluorinated isochroman isosteres.

Table 1: Reaction optimization.[a]

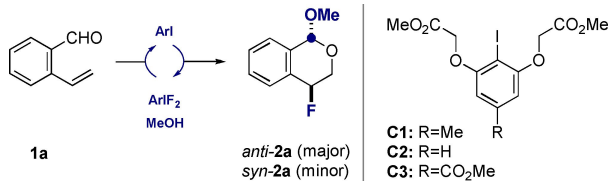

Entry	Solvent	Amine:HF	Cat.	MeOH [equiv]	Yield [%][b]
1	$CHCl_3$	1:4.5	C1	2.5	65
2	$CHCl_3$	1:4.5	C2	2.5	60
3	$CHCl_3$	1:4.5	C3	2.5	46
4	$CHCl_3$	1:4.5	C1	2.0	71
5	$CHCl_3$	1:4.5	C1	1.5	69
6	$CHCl_3$	1:4.0	C1	2.0	55
7	$CHCl_3$	1:5.0	C1	2.0	46
8	DCM	1:4.5	C1	2.0	57
9	DCE	1:4.5	C1	2.0	56
10	MeCN	1:4.5	C1	2.0	49
11[c]	$CHCl_3$	1:4.5	C1	2.0	78
12[d]	$CHCl_3$	1:4.5	C1	2.0	76
13[c,d]	$CHCl_3$	1:4.5	C1	2.0	85 (72)
14	$CHCl_3$	1:4.5	–	2.0	–
15	$CHCl_3$	1:4.5	C1	–	–
16[e]	$CHCl_3$	1:4.5	C1	2.0	–

[a] Standard reaction conditions: **1a** (0.2 mmol), Selectfluor® (1.5 equiv), amine·HF source prepared from NEt_3·3 HF and Olah's reagent (0.5 mL), solvent (0.5 mL), catalyst (20 mol%), MeOH (0.4 mmol), 24 h, rt. [b] Determined by ^{19}F NMR using ethyl 2-fluoroacetate as internal standard (*d.r.* ≥ 85:15). Combined yield. Combined isolated yield in parentheses. [c] Amine·HF mixture prepared with pyridine and Olah's reagent. [d] Amine·HF source (1.0 mL), solvent (1.0 mL). [e] No Selectfluor® was added.

Results and Discussion

To explore the feasibility of an I^{I}/I^{III} catalysis platform, the conversion of 2-vinylbenzaldehyde **1a** to 4-fluoro-1-methoxyisochroman **2a** was investigated (Table 1). To that end, the competence of resorcinol-based organocatalysts **C1–C3** to facilitate the desired reaction were examined using methanol for the acetalization. Initially, the reaction was performed with iodoresocinol-based catalyst **C1** (20 mol%), and MeOH (2.5 equiv), with Selectfluor® (1.5 equiv) functioning as the oxidant and amine·HF complex (1:4.5) as a nucleophilic fluoride source:[15] This would generate the requisite $ArIF_2$ species in situ.[16]

Since chlorinated solvents have proven to be excellent reaction media for I^{III}-based fluorination processes, $CHCl_3$ was initially chosen. The highly electron-rich iodoarene catalyst **C1** enabled product *anti*-**2a** to be generated in 65% yield (*d.r.* of 85:15). Employing the iodoresorcinol-derivatives **C2** and **C3** led to lower yields (entries 2 and 3). Reducing the equivalent of MeOH had a beneficial impact on the process (entries 4 and 5) and altering the Brønsted-acidity as a function of amine:HF ratio (entries 6 and 7)[17] confirmed that 1:4.5 was optimal. This ratio was adjusted by varying the amount of NEt_3·3 HF and Olah's reagent (see the Supporting Information). Altering the reaction medium did not lead to an enhancement in catalysis efficiency (entries 8–10). However, reducing the HF:pyridine ratio by adding more pyridine to Olah's reagent (entry 11), rather than of NEt_3·3 HF, and diluting the reaction mixture to a final concentration of 0.1 M (entry 12) led to improvements in the yield. Applying both changes simultaneously (entry 13), led to the highest yields of the optimization. Control reactions in the absence of catalyst, methanol and Selectfluor® did not generate the product (entries 14–16), supporting the involvement of an I^{I}/I^{III} catalysis pathway. Furthermore, altering the key reaction parameters listed in Table 1 had no significant impact on the diastereoselectivity of the reaction. As a control experiment, *anti*-**2a** was re-exposed to the reaction conditions and this resulted in the 85:15 equilibrium ratio being re-established. To explore the scope and limitations of the process, a series of substituted 2-vinylbenzaldehyes were exposed to the general fluorocyclization conditions using catalyst **C1** and methanol (Scheme 2). Leveraging these I^{I}/I^{III} catalysis conditions, it was possible to access a range of diversely substituted isochromans with diastereoselectivities up to >95:05 (*anti*:*syn*). Initially, the regiochemical impact of $C(sp^2)$-F fluorination on the aryl ring was explored. As it is evident from products **2b**–**2e**, the reaction proved to be insensitive to this series of structural modification (up to 84% yield). The methylated series **2f**–**2h** were also smoothly generated but this study revealed a, perhaps unsurprising, sensitivity towards steric alterations at the *ortho*-position (**2f**). Since products **2f** and **2g** decomposed under the standard reaction conditions, the amine:HF ratio was reduced to 1:4. In the chloro- (**2i**–**2k**, up to 97%) and bromo-series (**2l**–**2n**, up to 83%), the trend *ortho* < *meta* > *para* was noted. With a view to generating products that could be further functionalized, the tosylate **2o** was generated (72%) as was the

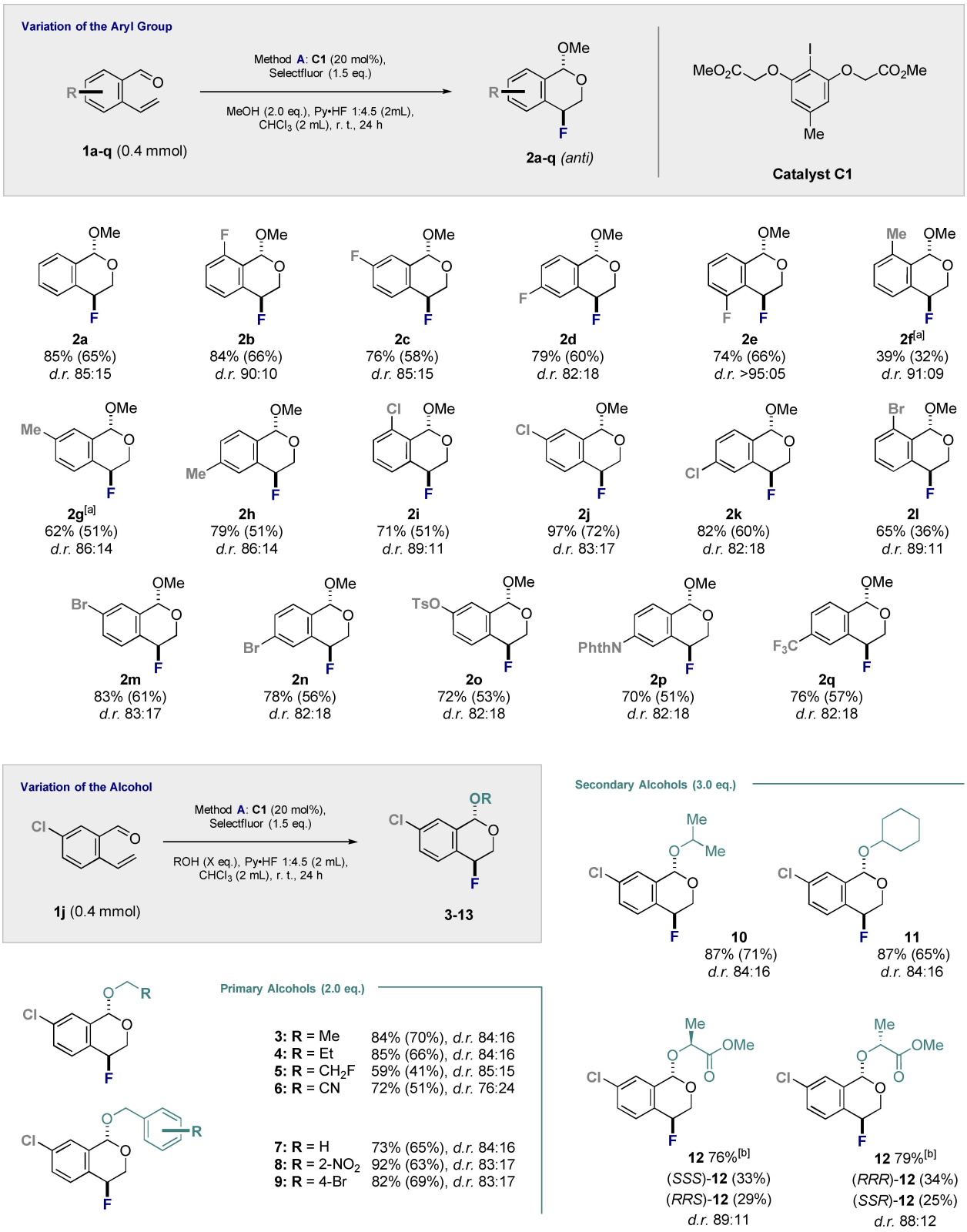

Scheme 2. Top: Scope for the fluorocyclization of 2-vinylbenzaldehydes **1** to the corresponding *anti*-4-fluoro-1-methoxyisochromanes **2**. Combined NMR yields are reported with isolated yields of the major isomer indicated in parentheses. Method **A**: 2-Vinylbenzaldehyde **1** (0.4 mmol), **C1** (20 mol%), $CHCl_3$ (2.0 mL), Py·HF 1:4.5 (2.0 mL), MeOH (0.8 mmol) and Selectfluor® (0.6 mmol), 24 h, room temperature. Bottom: Scope for the fluorocyclization of 5-chloro-2-vinylbenzaldehyde **1j** to the corresponding *anti*-4-fluoro-1-alkoxyisochromans **3**–**12**. The reported yields are combined NMR yields, isolated yields of the major isomer in parentheses. NB: For secondary alcohols, improved yields are observed by adding three equivalents of the corresponding alcohols. [a] Py·HF 1:4.0 (2.0 mL) was used. [b] Combined NMR yield of diastereoisomers.

masked aniline **2p** (70%). Cognizant of the popularity of the trifluoromethyl group in contemporary medicinal chemistry, product **2q** was prepared in 76% yield. To expand the scope of the process, the reaction of substrate **1j** with various primary alcohols to form *anti*-4-fluoro-1-alkoxyisochromans was investigated. Replacing methanol with ethanol and propanol proved unproblematic (**3** and **4**), as did the introduction of 2-fluoro and 2-cyano-ethanol to generate products **5** and **6**. Benzylic alcohols were also found to be effective coupling partners (compounds **7**–**9**), and can be considered as protected hemi-acetal derivatives. The addition of secondary alcohols in the scope was tolerated, and improved yields could be achieved by increasing the stoichiometry of the nucleophile added to three equivalents. Using isopropanol and cyclohexanol enabled products **10** and **11** to be prepared in 87% yield. Finally, to facilitate future large-scale access to optically pure products, the reaction was executed with both enantiomers of methyl lactate (compounds **12**, 76 and 79% yield, respectively).

Gratifyingly, compound **2a** was crystalline and it was possible to unequivocally establish the *anti*-relationship of the two stereocenters by single crystal X-ray diffraction (Figure 2). A pertinent feature of the analysis is the *quasi*-axial orientation of the C(sp^2)–O and C(sp^3)–F bonds, which is a manifestation of donor-acceptor $n_O \rightarrow \sigma^*_{C-O}$ and $\pi \rightarrow \sigma^*_{C-F}$ interactions,[1b] respectively (CCDC 2162683).[18] The latter interaction is clearly evident from the C(sp^3)–F bond length of 1.43 Å (cf 1.39 Å in CH_3F),[1b] and suggests that the CH_2-CHF unit functions as a stereoelectronic mimic of the O–CH(OR) acetal motif.

Having established a diastereoselective fluorocyclization route to the isochroman nucleus, the development of an enantioselective process was initiated. Since catalyst **C1** had proven to be highly effective, the *p*-TolI core was retained and advanced further (Table 2). Owing to the success of lactic acid-based side chains in I^I/I^{III} catalysis[19] and their ease of preparation and availability in both enantiomeric forms, the pendant glycolic acid chains were replaced with optically active modules to generate a C_2-symmetric environment. Gratifyingly, encouraging levels of enantioselectivity were noted using the methyl derivative (entry 1, 61:39 *e.r.*) under the standard conditions developed in Table 1. Replacing R^2 with Et and Bn did not lead to an improvement in catalysis (entries 2 and 3, respectively), thus

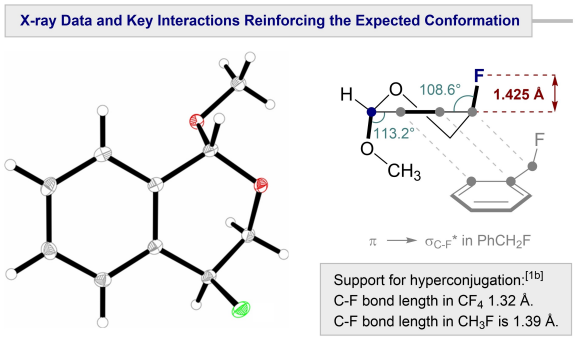

Figure 2. X-ray structural analysis of fluoroisochroman **2a**.[18]

Table 2: Enantioselective reaction optimization.[a]

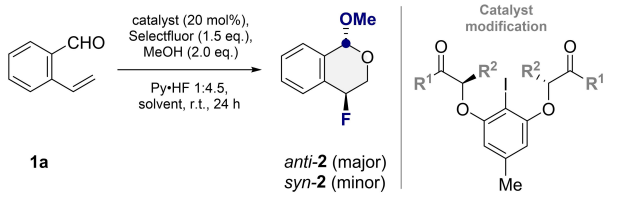

1a

anti-**2** (major)
syn-**2** (minor)

Entry	Solvent	R^1	R^2	Yield [%][b]	*e.r. anti*-**2a**
1	$CHCl_3$	OMe	Me	61	61:39
2	$CHCl_3$	OMe	Et	51	59:41
3	$CHCl_3$	OMe	Bn	40	56:44
4	$CHCl_3$	NMe_2	Me	57	63:37
5	$CHCl_3$	N(*i*-Pr)$_2$	Me	32	67:23
6	MeCN	N(*i*-Pr)$_2$	Me	54	81:19
7	MTBE	N(*i*-Pr)$_2$	Me	29	83:17
8	MeCN:MTBE 1:1	N(*i*-Pr)$_2$	Me	64	88:12
9	MeCN:MTBE 2:3	N(*i*-Pr)$_2$	Me	62	90:10
10[c]	MeCN:MTBE 2:3	N(*i*-Pr)$_2$	Me	66 (51)	90:10

[a] Standard reaction conditions: **1a** (0.2 mmol), Selectfluor® (1.5 equiv), amine·HF source prepared from pyridine and Olah's reagent (1.0 mL), solvent (1.0 mL), catalyst (20 mol%), MeOH (0.4 mmol), 24 h, rt. [b] Determined by ^{19}F NMR using ethyl 2-fluoroacetate as internal standard. Combined yield. Isolated yield of the major diastereoisomer in parentheses. [c] Solvent stored over molecular sieves.

subsequent modifications were performed at the carbonyl substituents (R^1). Replacing the esters by tertiary amides was investigated since this would mitigate concerns pertaining to hydrolytic stability and subsequent *trans*-esterification in more challenging reactions.[15] Whilst installing the dimethyl amide group had little impact on reaction efficiency or selectivity (entry 4), catalysis with the diisopropyl amide proved to be marginally more selective (entry 5). This could be further augmented by modifications to the reaction media, with a mixture of MeCN and MTBE ultimately leading to good levels of enantioselectivity (entries 6–9, up to 90:10 *e.r.*). A further yield enhancement was achieved when using solvents dried over molecular sieves (entry 10, Method **C**). Whereas the Brønsted-acidity of the system had to be lowered to prevent decomposition for the electron rich substrates **1f** and **1g** (Amine·HF 1:4.0, Method **B**), increased Brønsted-acidity was required for most of the halogenated substrates to guarantee full conversion after 24 h (Amine·HF 1:5.0, Method **D**). The optimized set of conditions was then applied to four sets of modified substrates to examine the impact of *ortho*-, *meta*- and *para*-substitution (Scheme 3).

Halogenated substrates were selected on account of their ease of post-reaction functionalization. In the fluorinated series (**2b**, **c**, **d**), *ortho*-substitution led to the highest *d.r.* of 93:07 with the *meta*- and *para*-derivatives performing comparably (89:11 and 84:16 *d.r.*, respectively). The highest levels of enantioselectivity were observed for the *para*-substituted system **2d** (97:03 *e.r.*). It is interesting to note that in the chlorinated series **2i**, **2j**, and **2k**, the diastereoselectivity followed a similar trend to the fluorinated systems. However, enantioselectivity showed little regio-dependence

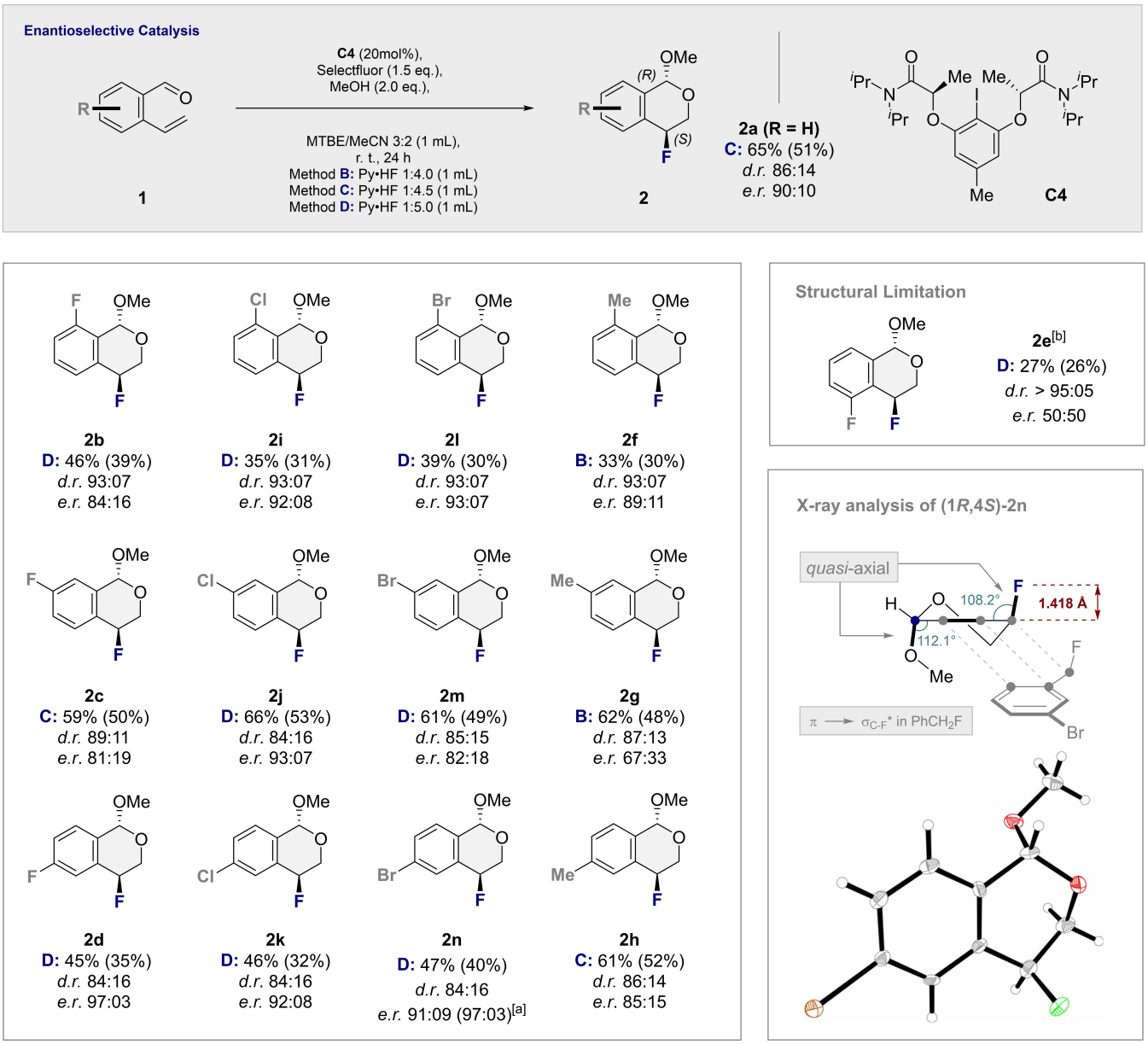

Scheme 3. Left: Scope for the fluorocyclization of 2-vinylbenzaldehydes **1** to the corresponding *anti*-4-fluoro-1-methoxyisochromanes **2**. The reported yields are combined NMR yields, isolated yields of the major isomer in parentheses. *e.r.* of the major diastereoisomer was determined by HPLC analysis and the *d.r. was* determined by ^{19}F NMR analysis of the crude reaction mixture. Method **B**: 2-Vinylbenzaldehyde **1** (0.2 mmol), **C4** (20 mol%), MTBE/MeCN 3:2 (1.0 mL), Py·HF 1:4.0 (1.0 mL), MeOH (0.4 mmol) and Selectfluor® (0.3 mmol), 24 h, room temperature. Method **C**: Py·HF 1:4.5 (1.0 mL) was used. Method **D**: Py·HF 1:5.0 (1.0 mL) was used. [a] After recrystallization. [b] The reaction time was increased to 48 h. Right: The X-ray crystal structure of compound (1*R*,4*S*)-**2n** (CCDC 2162684).

with compounds **2i**, **2j** and **2k** being generated with enantioselectivities of 92:08, 93:07 and 92:08 *e.r.*, respectively. In the brominated sequence (**2l**, **m**, **n**), the *ortho*-derivative was generated with high levels of enantio- and diastereoselectivity (93:07 *e.r.* and 93:07 *d.r.*). Although a slight decrease in *d.r.* was observed for the *meta*- and *para*-derivatives (85:15 and 84:16 for **2m** and **2n**, respectively), compound **2n** could be prepared with 91:09 *e.r.* and this could be further improved to 97:03 by simple recrystallization. In the methyl series, *ortho*-substitution was again well-tolerated (**2f**, 93:07 *d.r.* and 89:11 *e.r.*), whereas lower levels of stereo-control were noted for compounds **2g** and **2h**. In exploring the impact of substitution on the second non-equivalent *meta*-position (compound **2e**), a reduction in efficiency and *e.r.* was offset by excellent levels of diastereoselectivity (>95:05). Since the brominated compound **2n** was crystalline, it provided an opportunity to establish both the relative (*anti*) and absolute (1*R*,4*S*)- configuration of the product by single crystal diffraction (Scheme 3, inset right, (CCDC 2162684)).[20] As in the case of compound **2a** (Figure 2), the *quasi*-axial orientations of the C(sp^3)–F and C(sp^3)–O bonds in the half-chair allow for reinforcing,

stabilizing hyperconjugative interactions. The C–C–O and C–C–F angles of 112° and 108° reflect the balance that enables the stereoelectronic requirements for antiperiplanarity to be satisfied whilst minimizing 1,3-allylic strain[21] with the proximal C(sp^2)–H groups on the aryl ring. An elongated C(sp^3)–F bond length of 1.418 Å is in good agreement with compound **2a** (1.425 Å).

To rationalize the stereochemical outcome of this π-acid-mediated[22] fluorination step, a quadrant model is instructive in which coordination of the alkene occurs to the $A^{1,3}$-minimized catalyst (Figure 3). This is consistent with theoretical studies by Houk and Xue on related transformations.[23] Importantly, this induction model is supported by the catalyst editing studies shown in Table 2. These data demonstrate that as the steric bulk of large group (R^L) increases, so too does the enantioselectivity in the order $OMe < NMe_2 < N^iPr_2$. An inverse correlation was noted for the smaller group (R^S), with *e.r.* increases following the sequence Bn < Et < Me.

To demonstrate that the acetal component of the isochromans provides a functional handle for downstream manipulation, compound **2a** was converted to a selection of motifs that are commonly found in drug discovery campaigns (Scheme 4). Initially, the compound was exposed to difluorinated silyl enolether **A** in the presence of a Lewis acid additive. This example was selected on account of the bioisosteric nature of difluoromethylene unit as an ether surrogate (CF_2 versus O).[1b,4] Product **13** was isolated as an approximate 1:1 mixture of diastereoisomers with a combined yield of 90%. The *syn*-adduct was crystalline and it was possible to isolate crystals that were suitable for single crystal X-ray diffraction (CCDC 2162685).[24] This revealed that, even in the absence of the acetal motif, the C(sp^3)–F bond is *quasi*-axial and is an effective stereoelectronic mimic of the O–CH(OR) acetal.[25] This half-chair conformational preference is a manifestation of well-documented $\pi \rightarrow \sigma_{C-F}^*$ interactions.[1b,26] The exocyclic chain is also pre-organized to profit from reinforcing, antiperiplanar $\sigma_{C-O} \rightarrow \sigma_{C-F}^*$ and $\sigma_{C-H} \rightarrow \sigma_{C-F}^*$ interactions. Allylation with allyl-TMS in the presence of TMSOTf proved facile,[13] enabling the synthesis of compound **14** (89% yield) bearing a pendant alkene handle. As outlined in the introduction, the isochroman core is present in a plenum of bioactive small molecules including the selective D_4 receptor antagonist *Sonepiprazole*.[27] In a short synthetic sequence, it was possible to process compound **2a** to a selectively fluorinated analog (**17**) and to establish the relative configuration of the major diastereomer (CCDC 2162686).[28] Finally, cognizant that novel drug discovery modules are often required as solid precursors, a

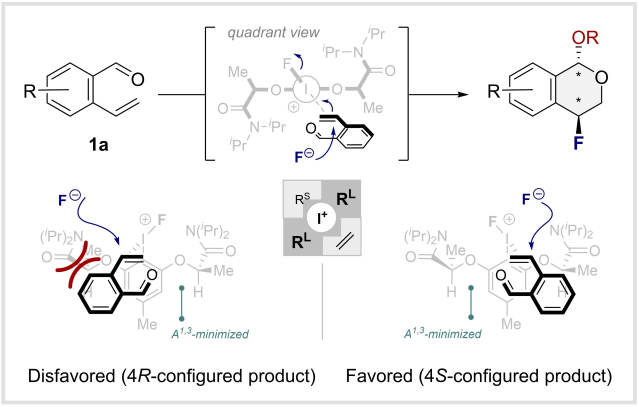

Figure 3. A postulated induction model to account for the formation of the (*S*)-configured fluorine center.

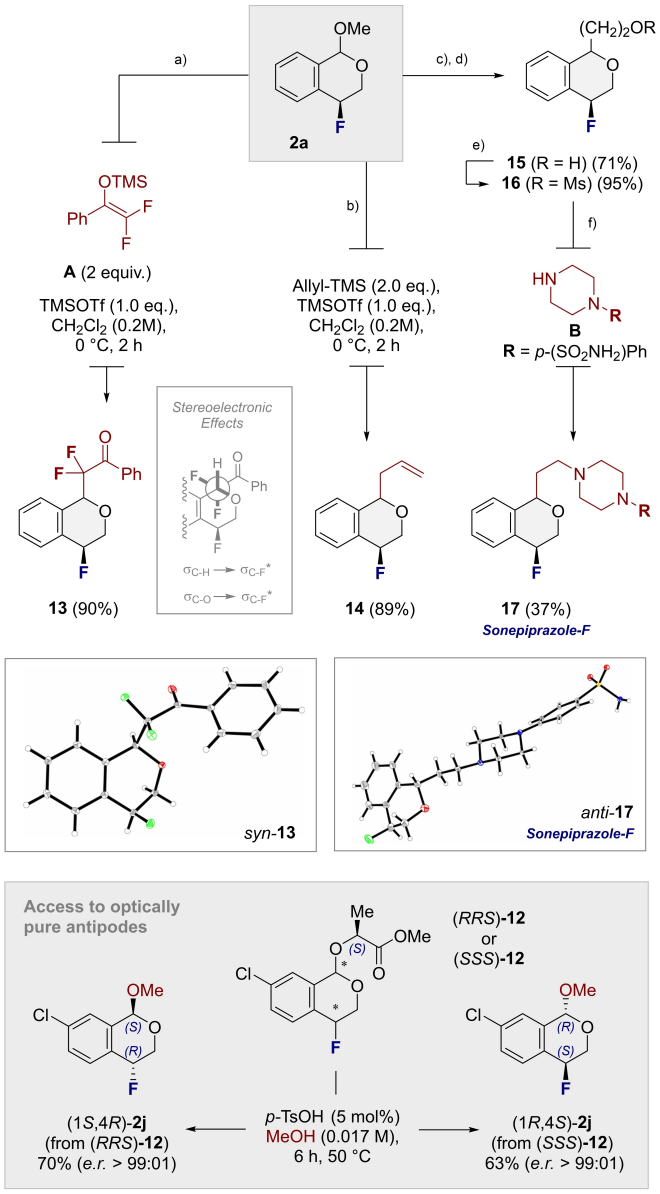

Scheme 4. Derivatization of fluoroisochroman **2a**. Conditions: a) **A** (2.0 equiv), TMSOTf (1.0 equiv), CH_2Cl_2 (0.2 M), 0 °C, 2 h. *syn*-**13** (48%), *anti*-**13** (42%). b) Allyl-TMS (2.0 equiv), TMSOTf (1.0 equiv), CH_2Cl_2 (0.2 M), 0 °C, 2 h. *Major*-**14** (55%), *minor*-**14** (34%). c) 2,2′-Bipy (3.0 equiv), TMSOTf (2.0 equiv), CH_2Cl_2 (0.2 M), 0 °C, 45 min., then VinylOTMS (1.05 equiv), DCM (0.2 M), 0 °C, 21 h. d) $NaBH_4$ (10.0 equiv), MeOH, 0 °C, 1.5 h. **15** (71% over 2 steps, *d.r.* 77:23). e) MsCl (1.05 equiv), DIPEA (1.1 equiv), CH_2Cl_2, 0 °C to rt, 1.5 h. **16** (95%, *d.r.* 77:23). f) **B** (1.1 equiv), DIPEA (1.4 equiv), ethylene glycol, 100 °C, 19 h. *Anti*-**17** (25%), *syn*-**17** (12%, *d.r.* 90:10).

facile hydrolysis protocol of (*RRS*)-**12** or (*SSS*)-**12** was developed that enabled both enantiomers [(1*S*,4*R*)-**2j** and (1*R*,4*S*)-**2j**] to be isolated in >99:01 *e.r.*

Conclusion

In the design of stereochemically defined bioisosteres and novel drug discovery modules, $I^{I/III}$ catalysis has emerged as a key enabling technology. Pendant carbonyl motifs have proven to be particularly effective but thus far have been limited to amides, esters and carboxylic acids. To this portfolio, it has been possible to add aldehydes, thereby integrating a third (σ-)bond forming event in the net transformation to generate additional structural complexity. In expanding this synthetic arsenal, novel fluoroisochromans can be generated in a single operation and with high levels of stereoselectivity (up to >95:05 *d.r.* and 97:03 *e.r.*). Not only does the benzylic fluoride shield an oxidatively labile position, X-ray analyses demonstrate that the [CH_2-CHF] fragment functions as a stereoelectronic mimic of the O-CH(OR) acetal motif. This reinforces the half chair conformation in the dominant 1,4-*anti*-product and retains this preference upon deletion of the acetal. Finally, the synthetic utility afforded by introduction of the acetal for subsequent downstream manipulations is showcased in the generation of a fluorinated analog of the highly selective D_4 receptor antagonist *Sonepiprazole* (**17**).

Acknowledgements

We acknowledge financial support from the WWU Münster, the Deutsche Forschungsgemeinschaft (SFB 858) and the European Research Council (ERC Consolidator Grant RECON 818949). Open Access funding enabled and organized by Projekt DEAL.

Conflict of Interest

The authors declare no conflict of interest.

Data Availability Statement

The data that support the findings of this study are available from the corresponding author upon reasonable request.

Keywords: Fluorination · Heterocycles · Hypervalent Iodine · Isosteres · Stereoelectronic Effects

[1] a) K. Müller, C. Faeh, F. Diederich, *Science* **2007**, *317*, 1881–1886; b) D. O'Hagan, *Chem. Soc. Rev.* **2008**, *37*, 308–319; c) D. O'Hagan, *J. Fluorine Chem.* **2010**, *131*, 1071–1081; d) L. E. Zimmer, C. Sparr, R. Gilmour, *Angew. Chem. Int. Ed.* **2011**, *50*, 11860–11871; *Angew. Chem.* **2011**, *123*, 12062–12074; e) J. Han, A. M. Remete, L. S. Dobson, L. Kiss, K. Izawa, H. Moriwaki, V. A. Soloshonok, D. O'Hagan, *J. Fluorine Chem.* **2020**, *239*, 109639; f) R. Mondal, M. Agbaria, Z. Nairoukh, *Chem. Eur. J.* **2021**, *27*, 7193–7213.

[2] For the discovery that fluorinated cortisone is more potent than the non-fluorinated systems, see: J. Fried, A. Borman, W. B. Kessler, P. Grabowich, E. F. Sabo, *J. Am. Chem. Soc.* **1958**, *80*, 2338–2339.

[3] a) F. Lovering, J. Bikker, C. Humblet, *J. Med. Chem.* **2009**, *52*, 6752–6756; b) P. A. Wender, B. L. Miller, *Nature* **2009**, *460*, 197–201; c) A. L. Hopkins, G. R. Bickerton, *Nat. Chem. Biol.* **2010**, *6*, 482–483; d) F. Lovering, *MedChemComm* **2013**, *4*, 515–519; e) D. C. Blakemore, L. Castro, I. Churcher, D. C. Rees, A. W. Thomas, D. W. Wilson, A. Wood, *Nat. Chem.* **2018**, *10*, 383–394; f) I. P. Silvestri, P. J. J. Colbon, *ACS Med. Chem. Lett.* **2021**, *12*, 1220–1229.

[4] a) S. Purser, P. R. Moore, S. Swallow, V. Gouverneur, *Chem. Soc. Rev.* **2008**, *37*, 320–330; b) N. A. Meanwell, *J. Med. Chem.* **2011**, *54*, 2529–2591; c) E. P. Gillis, K. J. Eastman, M. D. Hill, D. J. Donnelly, N. A. Meanwell, *J. Med. Chem.* **2015**, *58*, 8315–8359; d) Y. Zhou, J. Wang, Z. Gu, S. Wang, W. Zhu, J. L. Aceña, V. A. Soloshonok, K. Izawa, H. Liu, *Chem. Rev.* **2016**, *116*, 422–518; e) N. A. Meanwell, *J. Med. Chem.* **2018**, *61*, 5822–5880.

[5] a) A. J. Cresswell, S. T.-C. Eey, S. E. Denmark, *Angew. Chem. Int. Ed.* **2015**, *54*, 15642–15682; *Angew. Chem.* **2015**, *127*, 15866–15909; b) S. V. Kohlhepp, T. Gulder, *Chem. Soc. Rev.* **2016**, *45*, 6270–6288; c) I. G. Molnár, C. Thiehoff, M. C. Holland, R. Gilmour, *ACS Catal.* **2016**, *6*, 7167–7173; d) S. Meyer, J. Häfliger, R. Gilmour, *Chem. Sci.* **2021**, *12*, 10686–10695.

[6] a) R. Pratap, V. J. Ram, *Chem. Rev.* **2014**, *114*, 10476–10526. b) Tamanna, M. Kumar, K. Joshi, P. Chauhan, *Adv. Synth. Catal.* **2020**, *362*, 1907–1926.

[7] M. Inoue, Y. Sumii, N. Shibata, *ACS Omega* **2020**, *5*, 10633–10640.

[8] A. J. Kirby, *The Anomeric Effect and Related Stereoelectronic Effects at Oxygen*, Springer, New York, **1983**.

[9] G. Kerti, T. Kurtán, T.-Z. Illyés, K. E. Kövér, S. Sólyom, G. Pescitelli, N. Fujioka, N. Berova, S. Antus, *Eur. J. Org. Chem.* **2007**, 296–305.

[10] a) S. Wolfe, *Acc. Chem. Res.* **1972**, *5*, 102–111; b) D. Cahard, V. Bizet, *Chem. Soc. Rev.* **2014**, *43*, 135–147; c) C. Thiehoff, Y. P. Rey, R. Gilmour, *Isr. J. Chem.* **2017**, *57*, 92–100; d) M. Aufiero, R. Gilmour, *Acc. Chem. Res.* **2018**, *51*, 1701–1710.

[11] For selected reviews on I^{I}/I^{III} catalysis, see: a) A. Yoshimura, V. V. Zhdankin, *Chem. Rev.* **2016**, *116*, 3328–3435; b) X. Li, P. Chen, G. Liu, *Beilstein J. Org. Chem.* **2018**, *14*, 1813–1825; c) A. Claraz, G. Masson, *Org. Biomol. Chem.* **2018**, *16*, 5386–5402; d) A. Parra, *Chem. Rev.* **2019**, *119*, 12033–12088.

[12] Selected examples of fluorocyclization to generate oxygen-containing heterocycles, see a) W. Yuan, K. J. Szabó, *Angew. Chem. Int. Ed.* **2015**, *54*, 8533–8537; *Angew. Chem.* **2015**, *127*, 8653–8657; b) G. C. Geary, E. G. Hope, A. M. Stuart, *Angew. Chem. Int. Ed.* **2015**, *54*, 14911–14914; *Angew. Chem.* **2015**, *127*, 15124–15127; c) A. Ulmer, C. Brunner, A. M. Arnold, A. Pöthig, T. Gulder, *Chem. Eur. J.* **2016**, *22*, 3660–3664; d) E. M. Woerly, S. M. Banik, E. N. Jacobsen, *J. Am. Chem. Soc.* **2016**, *138*, 13858–13861; e) F. Scheidt, C. Thiehoff, G. Yilmaz, S. Meyer, C. G. Daniliuc, G. Kehr, R. Gilmour, *Beilstein J. Org. Chem.* **2018**, *14*, 1021–1027; f) A. Andries-Ulmer, C. Brunner, J. Rehbein, T. Gulder, *J. Am. Chem. Soc.* **2018**, *140*, 13034–13041; g) J. C. Sarie, C. Thiehoff, J. Neufeld, C. G. Daniliuc, R. Gilmour, *Angew. Chem. Int. Ed.* **2020**, *59*, 15069–15075; *Angew. Chem.* **2020**, *132*, 15181–15187; h) Q. Wang, M. Lübcke, M. Biosca, M. Hedberg, L. Eriksson, F. Himo, K. J. Szabó, *J. Am. Chem. Soc.* **2020**, *142*, 20048–20057.

[13] A. Matviitsuk, S. E. Denmark, *Angew. Chem. Int. Ed.* **2019**, *58*, 12486–12490; *Angew. Chem.* **2019**, *131*, 12616–12620.

[14] T. Charvillat, P. Bernardelli, M. Daumas, X. Pannecouke, V. Ferey, T. Besset, *Chem. Soc. Rev.* **2021**, *50*, 8178–8192.
[15] a) S. M. Banik, J. W. Medley, E. N. Jacobsen, *J. Am. Chem. Soc.* **2016**, *138*, 5000–5003; b) I. G. Molnár, R. Gilmour, *J. Am. Chem. Soc.* **2016**, *138*, 5004–5007.
[16] J. C. Sarie, C. Thiehoff, R. J. Mudd, C. G. Daniliuc, G. Kehr, R. Gilmour, *J. Org. Chem.* **2017**, *82*, 11792–11798.
[17] F. Scheidt, M. Schäfer, J. C. Sarie, C. G. Daniliuc, J. J. Molloy, R. Gilmour, *Angew. Chem. Int. Ed.* **2018**, *57*, 16431–16435; *Angew. Chem.* **2018**, *130*, 16669–16673.
[18] Deposition Number 2162683 (for **2a**) contains the supplementary crystallographic data for this paper. These data are provided free of charge by the joint Cambridge Crystallographic Data Centre and Fachinformationszentrum Karlsruhe Access Structures service.
[19] S. Haubenreisser, T. H. Wöste, C. Martínez, K. Ishihara, K. Muñiz, *Angew. Chem. Int. Ed.* **2016**, *55*, 413–417; *Angew. Chem.* **2016**, *128*, 422–426.
[20] Deposition Number 2162684 (for **2n**) contains the supplementary crystallographic data for this paper. These data are provided free of charge by the joint Cambridge Crystallographic Data Centre and Fachinformationszentrum Karlsruhe Access Structures service.
[21] R. W. Hoffmann, *Chem. Rev.* **1989**, *89*, 1841–1860.
[22] A. Fürstner, P. W. Davies, *Angew. Chem. Int. Ed.* **2007**, *46*, 3410–3449; *Angew. Chem.* **2007**, *119*, 3478–3519.
[23] B. Zhou, M. K. Haj, E. N. Jacobsen, K. N. Houk, X.-S. Xue, *J. Am. Chem. Soc.* **2018**, *140*, 15206–15218.
[24] Deposition Number 2162685 (for *syn*-**13**) contains the supplementary crystallographic data for this paper. These data are provided free of charge by the joint Cambridge Crystallographic Data Centre and Fachinformationszentrum Karlsruhe Access Structures service.
[25] J. Neufeld, T. Stünkel, C. Mück-Lichtenfeld, C. G. Daniliuc, R. Gilmour, *Angew. Chem. Int. Ed.* **2021**, *60*, 13647–13651; *Angew. Chem.* **2021**, *133*, 13760–13764.
[26] T. Schaefer, R. W. Schurko, R. Sebastian, F. E. Hruska, *Can. J. Chem.* **1995**, *73*, 816–825.
[27] R. E. TenBrink, C. L. Bergh, J. N. Duncan, D. W. Harris, R. M. Huff, R. A. Lahti, C. F. Lawson, B. S. Lutzke, I. J. Martin, S. A. Rees, S. K. Schlachter, J. C. Sih, M. W. Smith, *J. Med. Chem.* **1996**, *39*, 2435–2437.
[28] Deposition Number 2162686 (for *anti*-**17**) contains the supplementary crystallographic data for this paper. These data are provided free of charge by the joint Cambridge Crystallographic Data Centre and Fachinformationszentrum Karlsruhe Access Structures service.

Manuscript received: April 11, 2022
Accepted manuscript online: May 10, 2022
Version of record online: June 13, 2022